

RUSSIAN ACADEMY OF SCIENCE
Lenin Order of Siberian Branch
G.I. BUDKER INSTITUTE OF NUCLEAR PHYSICS

V.N. Baier and V.M. Katkov

OPPORTUNITY TO STUDY
THE LPM EFFECT IN ORIENTED CRYSTAL
AT GeV ENERGY

Budker INP 2007-34

Novosibirsk
2007

**Opportunity to study
the LPM effect in oriented crystal
at GeV energy**

V.N. Baier and V.M. Katkov

Institute of Nuclear Physics
630090, Novosibirsk, Russia

Abstract

The spectral distribution of electron-positron pair created by photon and the spectral distribution of photons radiated from high-energy electron in an oriented single crystal is calculated using the method which permits inseparable consideration both of the coherent and incoherent mechanisms of two relevant processes. The method includes the action of field of axis (or plane) as well as the multiple scattering of radiating electron or particles of the created pair (the Landau-Pomeranchuk-Migdal (LPM) effect). The influence of scattering on the coherent mechanism and the influence of field on the incoherent mechanism are analyzed. In tungsten, axis $\langle 111 \rangle$ for the pair creation process at temperature $T = 100$ K the LPM effect attains 8 % at photon energy 5 GeV and for the radiation process at $T = 293$ K the LPM effect reaches 6 % at electron energy 10 GeV.

1 Introduction

When the radiation formation length becomes comparable to the distance over which the multiple scattering becomes important, the probability of the bremsstrahlung process will be suppressed. This is the Landau-Pomeranchuk-Migdal (LPM) effect. The characteristic energy ε_e when the LPM effect affects the whole spectrum is

$$\varepsilon_e = \frac{m}{16\pi Z^2 \alpha^2 \lambda_c^3 n_a L_0}, \quad L_0 = \ln(ma) + \frac{1}{2} - f(Z\alpha), \quad a = \frac{111Z^{-1/3}}{m},$$
$$f(\xi) = \sum_{n=1}^{\infty} \frac{\xi^2}{n(n^2 + \xi^2)}, \quad (1)$$

where Z is the charge of nucleus, n_a is the mean atom density, $f(\xi)$ is the Coulomb correction. The energy ε_e is very high even for heavy elements: $\varepsilon_e = 2.73$ TeV for tungsten and $\varepsilon_e = 4.38$ TeV for lead.

The LPM effect was studied in SLAC E-146 experiment in many elements using electrons with energy 8 GeV and 25 GeV [1] and in CERN-SPS experiment in iridium Ir ($\varepsilon_e = 2.27$ TeV) and tantalum Ta ($\varepsilon_e = 3.18$ TeV) for electrons with energy up to 287 GeV [2]. The suppression of bremsstrahlung was observed in the soft part of spectrum $\omega \ll \varepsilon$. The LPM effect will manifest itself also in the process of electron-positron pair creation by a photon. In this process the characteristic photon energy $\omega_e = 4\varepsilon_e$. In contrast to the radiation process, where the LPM effect can be observed in soft part of spectrum, for observation of the effect in the pair creation process the energy $\omega \sim \omega_e$ is needed. No such energy is available for the time being. For description of the LPM effect including the discussion of mentioned experiments see e.g. review [3].

Recently authors developed a new approach to analysis of pair creation by a photon [4] and radiation from high energy electrons [5] in oriented crystals. This approach not only permits to consider simultaneously both the coherent and incoherent mechanisms of pair creation by a photon or photon emission from high energy electrons but also gives insight on influence of the LPM

effect on the considered mechanisms of pair creation or radiation in oriented crystals. The relative contribution of the LPM effect in total probability of pair creation Δ_p is found

$$\Delta_p = -\frac{W - W^{coh} - W^{inc}}{W}, \quad (2)$$

where W is the total probability of pair creation, W^{coh} is the total coherent probability of pair creation and W^{inc} is the total incoherent probability of pair creation. In tungsten crystal (axis $\langle 111 \rangle$) the relative contribution of the LPM effect attains $\Delta_p \simeq 5.5\%$ at the photon energy $\omega \simeq 7$ GeV for the temperature $T=100$ K and $\Delta_p \simeq 4.3\%$ at $\omega \simeq 12$ GeV for $T=293$ K [4]. The origin of the effect is connected with high effective density of atomic nuclei near the crystalline axis which can exceed the mean atom density by 3 order of magnitude. At higher photon energy the field action excludes the LPM effect. As opposed to the pair creation process where the coherent process is suppressed exponentially at the low photon energy, the coherent contribution to the radiation intensity is very essential for any electron energy. Because of this the relative contribution of the LPM effect into the total radiation intensity (the inverse radiation length) Δ_r (Δ_r is obtained from Δ_p by substitution of the probability W in Eq.(2) by the corresponding radiation intensity) is much smaller than in the pair creation probability: in tungsten crystal (axis $\langle 111 \rangle$) it has the maximum $\Delta_r \simeq 0.9\%$ at the electron energy $\varepsilon \simeq 0.3$ GeV for $T=100$ K and $\Delta_r \simeq 0.8\%$ at $\varepsilon \simeq 0.7$ GeV for $T=293$ K [5].

As it was mentioned, the LPM effect in an amorphous medium was observed in the radiation spectra. It turns out that in an oriented crystal the study of the pair creation spectrum (or the hard part of the radiation spectrum) is very convenient approach for the investigation of the LPM effect.

The study performed in the present paper is connected with experiment NA63 carried out recently at SPS at CERN (for proposal see [6]).

2 Spectrum of particles of a pair created by a photon

Basing on Eqs.(16) and (17) of [4] (see also Eq.(7.135) in [7]) we get the general expression for the spectral distribution of particles of pair created by a photon

$$\begin{aligned}
dW(\omega, y) &= \frac{\alpha m^2}{2\pi\omega} \frac{dy}{y(1-y)} \int_0^{x_0} \frac{dx}{x_0} G(x, y), \quad G(x, y) = \int_0^\infty F(x, y, t) dt + s_3 \frac{\pi}{4}, \\
F(x, y, t) &= \text{Im} \left\{ e^{f_1(t)} [s_2 \nu_0^2 (1 + ib) f_2(t) - s_3 f_3(t)] \right\}, \quad b = \frac{4\kappa_1^2}{\nu_0^2}, \quad y = \frac{\varepsilon}{\omega}, \\
f_1(t) &= (i-1)t + b(1+i)(f_2(t) - t), \quad f_2(t) = \frac{\sqrt{2}}{\nu_0} \tanh \frac{\nu_0 t}{\sqrt{2}}, \\
f_3(t) &= \frac{\sqrt{2}\nu_0}{\sinh(\sqrt{2}\nu_0 t)}, \tag{3}
\end{aligned}$$

where

$$s_2 = y^2 + (1-y)^2, \quad s_3 = 2y(1-y), \quad \nu_0^2 = 4y(1-y) \frac{\omega}{\omega_c(x)}, \quad \kappa_1 = y(1-y)\kappa(x), \tag{4}$$

ε is the energy of one of the created particles.

The situation is considered when the photon angle of incidence ϑ_0 (the angle between photon momentum \mathbf{k} and the axis (or plane)) is small $\vartheta_0 \ll V_0/m$. The axis potential (see Eq.(9.13) in [7]) is taken in the form

$$U(x) = V_0 \left[\ln \left(1 + \frac{1}{x + \eta} \right) - \ln \left(1 + \frac{1}{x_0 + \eta} \right) \right], \tag{5}$$

where

$$x_0 = \frac{1}{\pi d n_a a_s^2}, \quad \eta_1 = \frac{2u_1^2}{a_s^2}, \quad x = \frac{\varrho^2}{a_s^2}. \tag{6}$$

Here ϱ is the distance from axis, u_1 is the amplitude of thermal vibration, d is the mean distance between atoms forming the axis, a_s is the effective screening radius of the potential. The parameters in Eq.(5) were determined by means of fitting procedure, see Table 1.

The local value of parameter $\kappa(x)$ which determines the probability of pair creation in the field Eq.(5) is

$$\kappa(x) = -\frac{dU(\varrho)}{d\varrho} \frac{\omega}{m^3} = 2\kappa_s f(x), \quad f(x) = \frac{\sqrt{x}}{(x+\eta)(x+\eta+1)}, \quad \kappa_s = \frac{V_0\omega}{m^3 a_s} \equiv \frac{\omega}{\omega_s}. \tag{7}$$

For an axial orientation of crystal the ratio of the atom density $n(\varrho)$ in the vicinity of an axis to the mean atom density n_a is (see [4])

Table 1: Parameters of the pair photoproduction and radiation processes in the tungsten crystal, axis $\langle 111 \rangle$ and the germanium crystal, axis $\langle 110 \rangle$ for two temperatures T ($\varepsilon_0 = \omega_0/4$, $\varepsilon_m = \omega_m$, $\varepsilon_s = \omega_s$)

Crystal	T(K)	V_0 (eV)	x_0	η_1	η	ω_0 (GeV)	ε_m (GeV)	ε_s (GeV)	h
W	293	417	39.7	0.108	0.115	29.7	14.35	34.8	0.348
W	100	355	35.7	0.0401	0.0313	12.25	8.10	43.1	0.612
Ge	293	110	15.5	0.125	0.119	592	88.4	210	0.235
Ge	100	114.5	19.8	0.064	0.0633	236	50.5	179	0.459

$$\frac{n(x)}{n_a} = \xi(x) = \frac{x_0}{\eta_1} e^{-x/\eta_1}, \quad \omega_0 = \frac{\omega_e}{\xi(0)}, \quad \omega_e = 4\varepsilon_e = \frac{m}{4\pi Z^2 \alpha^2 \lambda_c^3 n_a L_0}. \quad (8)$$

The functions and values in Eqs.(3) and (4) are

$$\begin{aligned} \omega_c(x) &= \frac{\omega_e(n_a)}{\xi(x)g_p(x)} = \frac{\omega_0}{g_p(x)} e^{x/\eta_1}, \quad L = L_0 g_p(x), \\ g_p(x) &= g_{p0} + \frac{1}{6L_0} \left[\ln(1 + \kappa_1^2) + \frac{6D_p \kappa_1^2}{12 + \kappa_1^2} \right], \quad g_{p0} = 1 - \frac{1}{L_0} \left[\frac{1}{42} + h\left(\frac{u_1^2}{a^2}\right) \right], \\ h(z) &= -\frac{1}{2} [1 + (1+z)e^z \text{Ei}(-z)], \end{aligned} \quad (9)$$

where L_0 is defined in Eq.(1), the function $g_p(x)$ determines the effective logarithm using the interpolation procedure, $D_p = D_{sc} - 10/21 = 1.8246$, $D_{sc} = 2.3008$ is the constant entering in the radiation spectrum at $\chi/u \gg 1$ (or in electron spectrum in pair creation process at $\kappa_1 \gg 1$), see Eq.(7.107) in [7], $\text{Ei}(z)$ is the integral exponential function.

The expression for $dW(\omega, y)$ Eq.(3) includes both the coherent and incoherent contributions as well as the influence of the multiple scattering (the LPM effect) on the pair creation process (see [4]). The probability of the coherent pair creation is the first term ($\nu_0^2 = 0$) of the decomposition of Eq.(3) over ν_0^2 (compare with Eq.(12.7) in [7])

$$\begin{aligned} dW^{coh}(\omega, y) &= \frac{\alpha m^2}{2\sqrt{3}\pi\omega} \frac{dy}{y(1-y)} \int_0^{x_0} \frac{dx}{x_0} \left[2s_2 K_{2/3}(\lambda) + s_3 \int_\lambda^\infty K_{1/3}(z) dz \right], \\ \lambda = \lambda(x) &= \frac{2}{3\kappa_1}, \end{aligned} \quad (10)$$

where $K_\nu(\lambda)$ is MacDonald's function. The probability of the incoherent pair creation is the second term ($\propto \nu_0^2$) of the mentioned decomposition (compare with Eq.(21.31) in [7])

$$dW^{inc}(\omega, y) = \frac{4Z^2\alpha^3 n_a L_0}{15m^2} dy \int_0^\infty \frac{dx}{\eta_1} e^{-x/\eta_1} f(x, y) g_p(x), \quad (11)$$

where $g_p(x)$ is defined in Eq.(9),

$$\begin{aligned} f(x, y) &= f_1(z) + s_2 f_2(z), \quad f_1(z) = z^4 \Upsilon(z) - 3z^2 \Upsilon'(z) - z^3, \\ f_2(z) &= (z^4 + 3z) \Upsilon(z) - 5z^2 \Upsilon'(z) - z^3, \quad z = z(x, y) = \kappa_1^{-2/3}. \end{aligned} \quad (12)$$

Here

$$\Upsilon(z) = \int_0^\infty \sin\left(zt + \frac{t^3}{3}\right) dt \quad (13)$$

is the Hardy function.

The next terms of decomposition of the pair creation probability $dW = dW(\omega, y)$ over ν_0^2 describe the influence of multiple scattering on the pair creation process, the LPM effect. The third term ($\propto \nu_0^4$) of the mentioned decomposition has the form

$$\begin{aligned} \frac{dW^{(3)}(\omega, y)}{dy} &= -\frac{\alpha m^2 \omega \sqrt{3}}{5600 \pi \omega_0^2 x_0} \int_0^{x_0} \frac{g_p^2(x)}{\kappa(x)} \Phi(\lambda) e^{-2x/\eta_1} dx, \\ \Phi(\lambda) &= \lambda^2 (s_2 F_2(\lambda) - s_3 F_3(\lambda)), \\ F_2(\lambda) &= (7820 + 126\lambda^2) \lambda K_{2/3}(\lambda) - (280 + 2430\lambda^2) K_{1/3}(\lambda), \\ F_3(\lambda) &= (264 - 63\lambda^2) \lambda K_{2/3}(\lambda) - (24 + 3\lambda^2) K_{1/3}(\lambda), \end{aligned} \quad (14)$$

where λ is defined in Eq.(10).

We consider the case of relatively low photon energies where the influence of the field of axis on the pair creation process is still weak. In this case it is possible to single out the basic elements which distinguish the pair creation process in oriented crystal from the same process in amorphous medium. The first of these elements is the modification of the characteristic logarithm L_0 Eq.(1)

$$\ln a \rightarrow \ln a - h \left(\frac{u_1^2}{a^2} \right). \quad (15)$$

For $u_1 \ll a$ one has $h(u_1^2/a^2) \simeq -(1+C)/2 + \ln(a/u_1)$, $C = 0.577..$ and so this term characterizes the new value of upper boundary of impact parameters u_1 contributing to the value $\langle \mathbf{q}_s^2 \rangle$ instead of screening radius a in an amorphous medium (\mathbf{q}_s is the momentum transfer at random collision, see [4]).

Because to action of the field of axis the coherent pair creation by a photon process emerges at $\omega \sim \omega_m$. In near-threshold region the probability of this process has the form (see Eq.(12.14) in [7])

$$dW^{coh} = \frac{\alpha m^2 dy}{\omega_m x_0} \sqrt{-\frac{3f(x_m)}{4f''(x_m)}} \left(1 - \frac{s}{4}\right) \exp\left(-\frac{8}{3\kappa_m s}\right),$$

$$\kappa_m = \kappa(x_m) \equiv \frac{\omega}{\omega_m}, \quad \kappa'(x_m) = 0, \quad x_m = \frac{1}{6}(\sqrt{1+16\eta(1+\eta)} - 1 - 2\eta),$$

$$s = s(y) = 4y(1-y), \quad (16)$$

where the functions $f(x), \kappa(x)$ are defined in Eq.(7).

The correction to the probability of the incoherent pair creation in the region of the weak influence of the axis field is positive and the probability itself is

$$dW^{inc} = dW^{cr} \left[1 + \frac{5}{8}\sigma_1 s^2 \left(1 + \frac{7s}{150d}\right)\right]; \quad dW^{cr} = \frac{\alpha m^2 \eta_1 d}{\pi \omega_g x_0} dy, \quad \omega_g = \frac{\omega_0}{g_{p0}},$$

$$d = d(y) = 1 - \frac{s(y)}{3}, \quad \sigma_n = \sigma_n(\omega) = \int_0^{x_0} \kappa^2(x) \exp\left(-\frac{nx}{\eta_1}\right) \frac{dx}{\eta_1}, \quad (17)$$

where g_{p0} is defined in Eq.(9). Using Eq.(8) one has

$$dW^{cr} = \frac{\alpha m^2 \eta_1}{\pi \omega_0 x_0} d(y) g_{p0} dy = \frac{4Z^2 \alpha^3}{m^2} n_a L_0 d(y) g_{p0} dy. \quad (18)$$

If one omits in this expression the crystal summand in g_{p0} ($h(u_1^2/a^2)$), the probability dW^{cr} will be very close to the Bethe-Maximon probability.

The expression Eq.(14) for $dW^{(3)}/dy$ contains the same near-threshold smallness as in Eq.(16) and additionally the small factor ν_0^4 . Because of this one can neglect this term in the region of applicability of Eqs.(16),(17).

The next terms of decomposition of the pair creation probability $dW = dW(\omega, y)$ over ν_0^2 in the region under study is

$$\frac{dW^{(4)}}{dy} = -\frac{dW^{cr}}{dy} \frac{\omega^2 s^2}{3\omega_g^2} \left[\left(1 + \frac{5s}{63d}\right) \left(1 + \frac{377}{16}\sigma_3 s^2\right) - \frac{1651\sigma_3 s^2 s_2}{10080d} \right]. \quad (19)$$

The last equation, which describes the LPM effect in the region of weak influence of the field, has the rather narrow region of applicability because of the large coefficient $377/16$ in front of depending on the field correction. Let us note that one can use following simple expressions for the entering $\sigma_{1,3}$

$$\sigma_1 \simeq \frac{3}{4} \left(\frac{\omega}{\omega_m} \right)^2, \quad \sigma_3 \simeq \frac{3}{14} \left(\frac{\omega}{\omega_m} \right)^2, \quad (20)$$

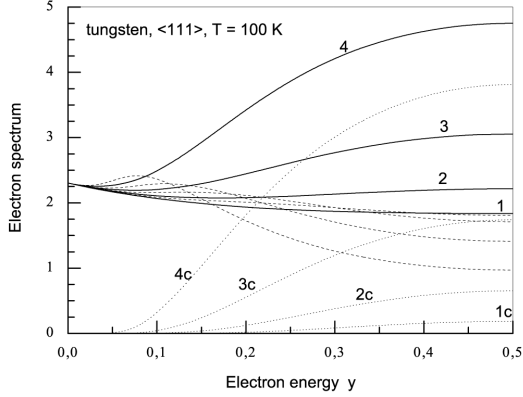
without violating the accuracy of derived above approximate probabilities.

The different contributions to the spectra of created pair (in units cm^{-1}) in tungsten, axis $< 111 >$, temperature $T=100$ K, for the energies where the coherent and the incoherent contributions are comparable, are shown in Fig.1(a), where one-half of spectra, which are symmetric with respect of the line $y = 0.5$, are shown. Let us discuss the spectra. When one of the created particles is soft $y \ll 1$ (the other particle takes the large part of photon energy) the incoherent contributions dominate. For $\kappa_m \geq 1$ and at $y \ll 1/\kappa_m$ this part of the spectrum is described by Eqs.(16), (17). With y increase the coherent contributions appear. Their relative contributions to the summary spectra grow fast with photon energy increase: if for $\omega = 5$ GeV (the lowest considered energy) the coherent contribution is rather small, then for $\omega = 15$ GeV (the highest considered energy) the coherent contribution dominates at $y \sim 0.5$. In this region the incoherent contributions decrease. This reduction becomes more essential with photon energy increase. For $\omega = 7$ GeV the interplay of the coherent and incoherent contributions is leading to the nearly flat final spectrum (the variation is less than 10%, this is quite unusual). It should be noted that for $\omega = 7$ GeV the right end ($y = 0.5$) is slightly lower than the left end of spectrum ($y \rightarrow 0$): $dW/dy(y \rightarrow 0) = 2.303 \text{ cm}^{-1}$ and $dW(y = 0.5) = 2.215 \text{ cm}^{-1}$, while the sum of the incoherent and coherent contributions is slightly higher: $dW^{inc}/dy(y = 0.5) + dW^{coh}/dy(y = 0.5) = 2.365 \text{ cm}^{-1}$. The arising difference is the consequence of the LPM effect. This property may be very useful in experimental study.

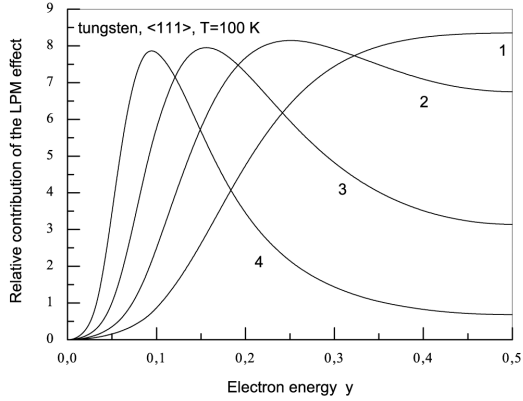
We define the contribution of the LPM effect into the spectral distribution of created pair, by analogy with [4], as

$$\Delta_p(\omega, y) = - \frac{dW(\omega, y) - dW^{coh}(\omega, y) - dW^{inc}(\omega, y)}{dW(\omega, y)}. \quad (21)$$

The function $\Delta_p(\omega, y)$ is shown in Fig.1(b). It reaches the highest value $\Delta_p = 8.35 \%$ at $\omega = 5$ GeV and $y = 0.5$. At $\omega = 7$ GeV the maximal value $\Delta_p = 8.15\%$ is attained at $y = 0.24$, at $\omega = 10$ GeV the maximal value



(a)

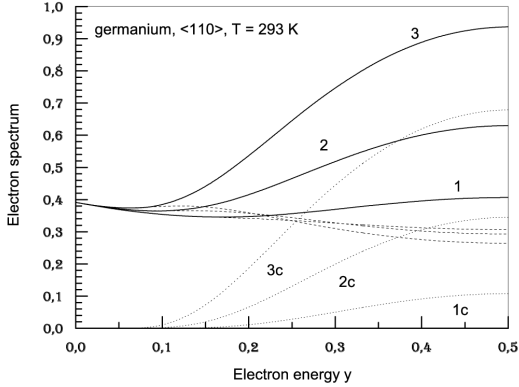


(b)

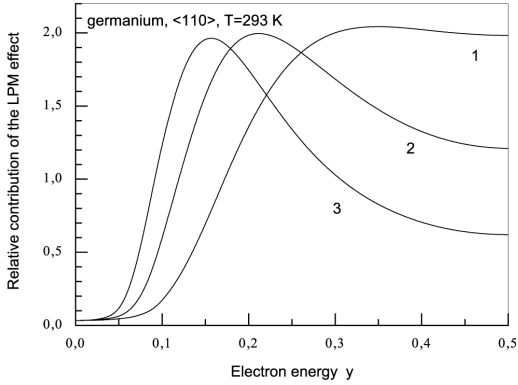
Figure 1: The spectral distribution of created by a photon pair vs the electron energy $y = \varepsilon/\omega$ in tungsten, axis $\langle 111 \rangle$, temperature $T=100$ K.

(a) The different contributions to the electron (positron) spectrum (in units cm^{-1}) The curves 1, 2, 3, 4 are the theory prediction $dW(\omega, y)/dy$ (see Eq.(3)) for photon energies $\omega = 5, 7, 10, 15$ GeV respectively, The dotted curves 1c, 2c, 3c, 4c are the corresponding coherent contributions $dW^{coh}(\omega, y)/dy$, the dashed curves present the incoherent contributions $dW^{inc}(\omega, y)/dy$. At $y \rightarrow 0.5$ these curves from top to bottom are correspondingly for the photon energies $\omega = 5, 7, 10, 15$ GeV.

(b) The relative contribution of the LPM effect in the spectral distribution of created electron (see Eq.(14)) $\Delta_p(\omega, y)$ (per cent). The curves 1, 2, 3, 4 are correspondingly for photon energies $\omega = 5, 7, 10, 15$ GeV.



(a)



(b)

Figure 2: The spectral distribution of created by a photon pair vs the electron energy $y = \varepsilon/\omega$ in germanium, axis $\langle 110 \rangle$, temperature $T=293$ K.

(a) The different contributions to the electron (positron) spectrum (in units cm^{-1}) The curves 1, 2, 3, are the theory prediction $dW(\omega, y)/dy$ (see Eq.(3)) for photon energies $\omega = 55, 75, 95$ GeV respectively, The dotted curves 1c, 2c, 3c are the corresponding coherent contributions $dW^{coh}(\omega, y)/dy$, the dashed curves present the incoherent contributions $dW^{inc}(\omega, y)/dy$. At $y \rightarrow 0.5$ these curves from top to bottom are correspondingly for the photon energies $\omega = 55, 75, 95$ GeV.

(b) The relative contribution of the LPM effect in the spectral distribution of created electron (see Eq.(14)) $\Delta_p(\omega, y)$ (per cent). The curves 1, 2, 3 are correspondingly for photon energies $\omega = 55, 75, 95$ GeV.

$\Delta_p = 8\%$ is attained at $y = 0.16$, and at $\omega = 15$ GeV the maximal value $\Delta_p = 7.86\%$ is attained at $y = 0.09$.

The same characteristics but for germanium, axis $< 110 >$, $T = 293$ K are shown in Fig.2. In this case the nearly flat spectrum appears at $\omega = 55$ GeV. The LPM effect is essentially weaker: at $\omega = 55$ GeV the maximal value $\Delta_p = 2.04\%$ is attained at $y = 0.34$, at $\omega = 75$ GeV the maximal value $\Delta_p = 2\%$ is attained at $y = 0.22$, and at $\omega = 95$ GeV the maximal value $\Delta_p = 1.98\%$ is attained at $y = 0.16$.

All the curves in Figs.1(b) and 2(b) have nearly the same height of the maximum and the position of the maximum y_m can be found roughly by solving the equation $s(y_m) = 2\omega_m/3\omega$ (the function $s(y)$ is defined in Eq.(16)). Since $s(y_m) \leq 1$ one has from the equation the boundary value of the photon energy $\omega_b \simeq 2\omega_m/3$. For higher photon energy the value $\Delta_p(\omega, y)$ varies insignificantly. At $\omega \ll \omega_b$ the value $\Delta_p^{max} = \Delta_p(\omega, 1/2)$ decreases as ω^2 with ω reduction according to Eq.(19)). The absolute maximum of the LPM effect is achieved at $\omega = \omega_b$ and $y = 1/2$. Since at $\omega \geq \omega_b$ Eq.(19)) is unapplicable at $y = y_m$ (in the maximum of the LPM effect the depending on field correction is large $((377/16)\sigma_3(\omega)s^2(y_m) \simeq 5s^2(y_m)\kappa_m^2 \simeq 2)$, so Eq.(19)) can be used for rough estimates only: $\Delta_p^{max} \sim \omega_m^2/3\omega_g^2$. For tungsten, $T=100$ K one has $\omega_m/\omega_g \simeq 0.54$, so that $\Delta_p^{max} \sim 9\%$ (in reasonable agreement with Fig.1(b)); the position estimates according to the presented scheme are in good agreement with Fig.1(b). For tungsten, $T=293$ K one has $\omega_m/\omega_g \simeq 0.43$, so that $\Delta_p^{max} \sim 6\%$; the numerical calculation in frame of the developed theory gives for the pair (Δ_p, y_m) the following results: for $\omega = 10$ GeV (6.6%, 0.36), for $\omega = 15$ GeV (6.4%, 0.18), for $\omega = 25$ GeV (6.3%, 0.1). The position estimates according to presented scheme are in reasonable agreement with these data. For germanium, $T=293$ K one has $\omega_m/\omega_g \simeq 1/7$, so the magnitude of the LPM is essentially smaller. Small magnitude of the LPM effect for light and intermediate elements was discussed in [3].

3 Spectrum of radiation from high-energy electron

The expression for the spectral probability of radiation used in the above derivation can be found from the spectral distribution Eq.(3) ($dW/dy = \omega dW/d\varepsilon$) using the standard QED substitution rules: $\varepsilon \rightarrow -\varepsilon$, $\omega \rightarrow -\omega$, $\varepsilon^2 d\varepsilon \rightarrow \omega^2 d\omega$ and exchange $\omega_c(x) \rightarrow 4\varepsilon_c(x)$. As a result one has

for the spectral intensity $dI = \omega dW$

$$dI(\varepsilon, y_r) = \frac{\alpha m^2}{2\pi} \frac{y_r dy_r}{1 - y_r} \int_0^{x_0} \frac{dx}{x_0} G_r(x, y_r), \quad G_r(x, y_r) = \int_0^\infty F_r(x, y_r, t) dt - r_3 \frac{\pi}{4},$$

$$F_r(x, y_r, t) = \text{Im} \left\{ e^{\varphi_1(t)} \left[r_2 \nu_{0r}^2 (1 + ib_r) f_2(t) + r_3 f_3(t) \right] \right\}, \quad b_r = \frac{4\chi^2(x)}{u^2 \nu_{0r}^2},$$

$$y_r = \frac{\omega}{\varepsilon}, \quad u = \frac{y_r}{1 - y_r}, \quad \varphi_1(t) = (i - 1)t + b_r(1 + i)(f_2(t) - t), \quad (22)$$

where

$$r_2 = 1 + (1 - y_r)^2, \quad r_3 = 2(1 - y_r),$$

$$\nu_{0r}^2 = \frac{1 - y_r}{y_r} \frac{\varepsilon}{\varepsilon_c(x)}, \quad (23)$$

where the functions $f_2(t)$ and $f_3(t)$ are defined in Eq.(3). The local value of parameter $\chi(x)$ which determines the radiation probability in the field Eq.(5) is

$$\chi(x) = -\frac{dU(\varrho)}{d\varrho} \frac{\varepsilon}{m^3} = 2\chi_s f(x), \quad \chi_s = \frac{V_0 \varepsilon}{m^3 a_s} \equiv \frac{\varepsilon}{\varepsilon_s}, \quad (24)$$

where $f(x)$ is defined in Eq.(7).

The functions and values in Eqs.(22) and (23) (see also Eqs.(8) and (9)) are

$$\varepsilon_c(x) = \frac{\varepsilon_e(n_a)}{\xi(x) g_r(x)} = \frac{\varepsilon_0}{g_r(x)} e^{x/\eta_1},$$

$$g_r(x) = g_{r0} + \frac{1}{6L_0} \left[\ln \left(1 + \frac{\chi^2(x)}{u^2} \right) + \frac{6D_r \chi^2(x)}{12u^2 + \chi^2(x)} \right],$$

$$g_{r0} = 1 + \frac{1}{L_0} \left[\frac{1}{18} - h \left(\frac{u_1^2}{a^2} \right) \right], \quad (25)$$

where the function $g_r(x)$ determines the effective logarithm using the interpolation procedure: $L = L_0 g_r(x)$, see Eq.(9), $D_r = D_{sc} - 5/9 = 1.7452$.

The expression for dI Eq.(22) includes both the coherent and incoherent contributions as well as the influence of the multiple scattering (the LPM effect) on the photon emission process (see [5]). The intensity of the coherent radiation is the first term ($\nu_0^2 = 0$) of the decomposition of Eq.(22) over ν_{0r}^2

(compare with Eq.(17.7) in [7])

$$dI^{coh}(\varepsilon, y_r) = \frac{\alpha m^2 y_r dy_r}{\sqrt{3}\pi} \int_0^{x_0} \frac{dx}{1-y_r} \left[r_2 K_{2/3}(\lambda_r) - (1-y_r) \int_{\lambda_r}^{\infty} K_{1/3}(z) dz \right],$$

$$\lambda_r = \lambda_r(x) = \frac{2u}{3\chi(x)}. \quad (26)$$

The intensity of the incoherent radiation is the second term ($\propto \nu_0^2$) of the mentioned decomposition (compare with Eq.(21.21) in [7])

$$dI^{inc}(\varepsilon, y_r) = \frac{\alpha m^2 \varepsilon}{60\pi \varepsilon_0} dy_r \int_0^{\infty} \frac{dx}{x_0} e^{-x/\eta_1} f_r(x, y_r) g_r(x), \quad (27)$$

where

$$f_r(x, y_r) = [y_r^2(f_1(z) + f_2(z)) + 2(1-y_r)f_2(z)],$$

$$z = \left(\frac{u}{\chi(x)} \right)^{2/3}, \quad (28)$$

the functions $f_{1,2}(z)$ are defined in Eq.(12).

The next terms of decomposition of for the spectral intensity of radiation $I(\varepsilon, y_r)$ over ν_{0r}^2 describe the influence of multiple scattering on the photon emission process, the LPM effect. The third term ($\propto \nu_{0r}^4$) of the mentioned decomposition has the form

$$dI^{(3)}(\varepsilon, y_r) = -\frac{\alpha m^2 \sqrt{3}}{89600\pi x_0} dy_r \left(\frac{\varepsilon}{\varepsilon_0} \right)^2 \int_0^{x_0} \frac{g_r^2(x)}{\chi(x)} \Phi(\lambda_r(x)) e^{-2x/\eta_1} dx, \quad (29)$$

where

$$\Phi(\lambda_r) = \lambda_r^2(r_2 F_2(\lambda_r) + r_3 F_3(\lambda_r)), \quad (30)$$

where λ_r is defined in Eq.(26), the functions F_2 and F_3 are defined in Eq.(14).

When $\chi_m = \chi(x_m) \equiv \varepsilon/\varepsilon_m \leq 1$ (see Eq.(16)) and the emitted photon is soft enough ($y_r \ll \chi_m$) Eqs.(17.11)-(17.13) in [7] may be used. For $\vartheta_0 = 0$ and $u \simeq y_r \ll 1$ one has the following expression

$$\frac{dI^{coh}}{d\omega} = \left(\frac{2}{\sqrt{3}} \right)^{5/3} \Gamma \left(\frac{2}{3} \right) \frac{\alpha m^2}{\pi x_0 \varepsilon_s} \left(\frac{y_r}{\chi_s} \right)^{1/3} \left(\ln \left(\frac{\chi_s}{y_r} \right) + a(\eta) \right), \quad (31)$$

where

$$a = a(\eta) = \ln(18\sqrt{3}) - \frac{\pi}{2\sqrt{3}} - C - \frac{3}{4} - l_1(\eta), \quad C = 0.577\dots \quad (32)$$

$$l_1(\eta) = 3.975\beta^{2/3} \left(1 + \frac{8\beta}{15} + \frac{7\beta^2}{18} \right) - \beta \left(\frac{3}{2} + \frac{9\beta}{8} + \frac{13\beta^2}{14} \right), \quad \beta = \frac{\eta}{1+\eta}.$$

The position of the maximum y_{rm} of this contribution and its value are given by the expressions

$$y_{rm} = \exp(-3 - a(\eta))\chi_s, \quad \frac{dI^{coh}(y_{rm})}{d\omega} \simeq \frac{8\varepsilon_0}{\varepsilon_s\eta_1 L_{rad}} \left(1 + \frac{2}{3}a \right) e^{-a/3}, \quad (33)$$

where L_{rad} is the Bethe-Maximon radiation length, see e.g. Eq.(7.54) in [7].

On the same assumptions the contribution of the incoherent radiation is (see Eq.(7.107) in [7])

$$\begin{aligned} \frac{dI^{inc}}{d\omega} &= \Gamma\left(\frac{1}{3}\right) \frac{1}{5L_{rad}} \int_0^{x_0} \left(\frac{y_r}{3\chi(x)} \right)^{2/3} \left[g_{r0} + \frac{1}{L_0} \left(D_r + \frac{1}{3} \ln \frac{\chi(x)}{y_r} \right) \right] e^{-x/\eta_1} \frac{dx}{\eta_1} \\ &\simeq 0.3L_{rad}^{-1} \left(\frac{y_r}{\chi_m} \right)^{2/3} \left[g_{r0} + \frac{1}{L_0} \left(\frac{5}{3} + \frac{1}{3} \ln \frac{\chi_m}{y_r} \right) \right]. \end{aligned} \quad (34)$$

In the maximum of the spectral distribution this contribution can be written as

$$\frac{dI^{inc}}{d\omega} \simeq 0.04 \left(\frac{\varepsilon_m}{\varepsilon_s} \right)^{2/3} e^{-2a/3} \left[g_{r0} + \frac{1}{L_0} \left(\frac{8}{3} + \frac{a}{3} + \frac{1}{3} \ln \frac{\varepsilon_s}{\varepsilon_m} \right) \right] L_{rad}^{-1}, \quad (35)$$

and it is very small comparing with the coherent one.

In the case of weak influence of the axis field the intensity spectrum of the incoherent radiation has the form

$$\begin{aligned} \frac{dI^{inc}}{d\omega} &\simeq \frac{dI^{cr}}{d\omega} \left[1 + \frac{15}{2} \left(\frac{\chi_m}{u} \right)^2 \left(1 - \frac{14}{75} \frac{(1-y_r)}{d_r(y_r)} \right) \right], \quad d_r(y_r) = y_r^2 + \frac{4}{3}(1-y_r), \\ \frac{dI^{cr}}{d\omega} &= \frac{\alpha m^2 \eta_1}{4\pi x_0} \frac{\varepsilon}{\varepsilon_g} d_r(y_r), \quad \varepsilon_g = \frac{\varepsilon_0}{g_{r0}}, \end{aligned} \quad (36)$$

where the value g_{r0} is defined in Eq.(25), u is defined in Eq.(22). Using Eqs.(8), (9), (25) one has

$$\frac{dI^{cr}}{d\omega} = \frac{4Z^2\alpha^3}{m^2} n_a L_0 d_r(y_r) g_{r0} = L_{rad}^{-1} \left(g_{r0} - \frac{1}{18L_0} \right) d_r(y_r). \quad (37)$$

If one omits in this expression the crystal summand in g_{r0} ($h(u_1^2/a^2)$), the intensity dI^{cr} will be very close to the Bethe-Maximon one (see also Eq.(18)). In this case the coherent contribution is

$$\frac{dI^{coh}}{d\omega} = \frac{\alpha m^2 x_m \sqrt{3}}{\varepsilon_m x_0} (1 - y_r + y_r^2) e^{-2u/3\chi_m}, \quad (38)$$

where x_m is defined in Eq.(16).

The next terms of decomposition of the radiation intensity $dI = dI(\varepsilon, y_r)$ over ν_0^2 which defines the LPM effect (compare with Eq.(19)) is

$$\frac{dI^{(4)}}{d\omega} \simeq \frac{dI^{cr}}{d\omega} \frac{\varepsilon^2}{3u^2\varepsilon_g^2} \left(1 - \frac{20}{63} \frac{(1 - y_r)}{d_r(y_r)} \right) \left(1 + 80 \frac{\chi_m^2}{u^2} \right). \quad (39)$$

The last expression has rather narrow interval of applicability because of large coefficient 80 in front of depending on field correction. In Eq.(38) we used the simple estimate $-4f''(x_m)/f(x_m) \simeq 1/x_m^2$ ($x_m \simeq \eta \ll 1$) and in Eqs.(36) and (39) we used Eq.(20) without violating accuracy of derived above approximate expressions.

The spectra of radiation from an electron in tungsten, axis $\langle 111 \rangle$, temperature $T=293$ K, for the energies where the coherent $I^{coh}(\varepsilon)$ and the incoherent $I^{inc}(\varepsilon)$ contributions to the total intensity are comparable, are shown in Fig.3(a). These spectra describe radiation in thin targets where one can neglect the energy loss of projectile. Weak variation of the spectral intensity of radiation near the maximum in the soft part of spectrum is described quite satisfactory by Eqs.(31), (33). Although it is quite difficult to determine the position of the maximum within a good accuracy, its height is given by Eq.(33) with precision better 10 %. It is seen that the phenomena under consideration become apparent at relatively low energy. For $\varepsilon = 1$ GeV, $dI^{coh} \simeq dI^{inc}$ at $y_r = y_c \simeq 0.2$ ($\omega \simeq 200$ MeV) while for lower photon energy the coherent contribution dominates and for higher photon energy the incoherent contribution dominates. For $\varepsilon = 3$ GeV, $dI^{coh} \simeq dI^{inc}$ at $y_r = y_c \simeq 0.42$ ($\omega \simeq 1.26$ GeV), for $\varepsilon = 5$ GeV, $dI^{coh} \simeq dI^{inc}$ at $y_r = y_c \simeq 0.54$ ($\omega \simeq 2.7$ GeV), and for $\varepsilon = 10$ GeV, $dI^{coh} \simeq dI^{inc}$ at $y_r = y_c \simeq 0.7$ ($\omega \simeq 7$ GeV). One can estimate the position $y_c(u_c = y_c/(1+y_c))$ using Eq.(38)

$$\frac{dI^{coh}}{d\omega}(u = u_c) \sim \frac{\alpha m^2 \eta_1 \sqrt{3}}{\varepsilon_m x_0} e^{-2u_c/3\chi_m} = L_{rad}^{-1} = \frac{\alpha m^2 \eta_1}{4\pi \varepsilon_0 x_0}, \quad u_c = \frac{3\varepsilon}{2\varepsilon_m} \ln \frac{4\pi\sqrt{3}\varepsilon_0}{\varepsilon_m}. \quad (40)$$

The values of y_c calculated according Eq.(40) are in a good agreement with Fig.3(a).

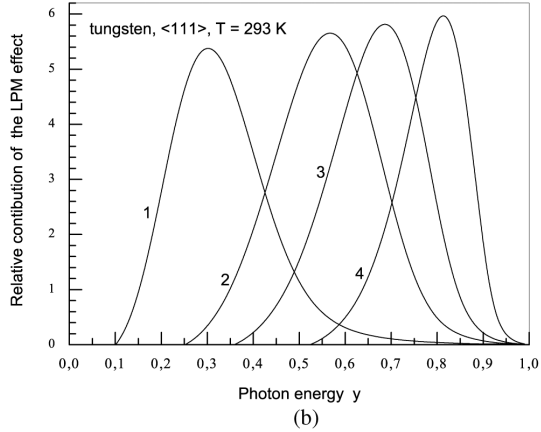
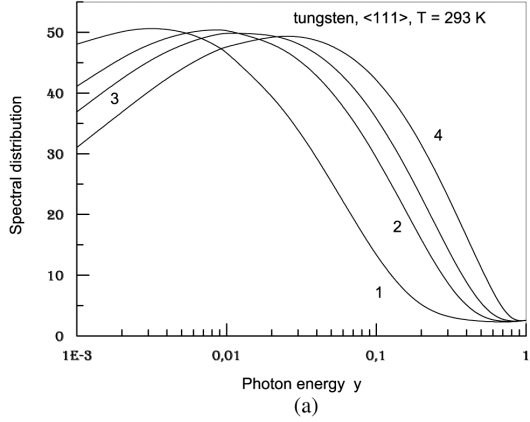


Figure 3: The radiation spectral intensity vs the photon energy $y = \omega/\varepsilon$ in tungsten, axis $\langle 111 \rangle$, temperature $T=293$ K.

(a) The intensity distribution $dI(\varepsilon, y_r)/d\omega$ (in units cm^{-1}) The curves 1, 2, 3, 4 are the theory prediction (see Eq.(22)) for electron energies $\varepsilon = 1, 3, 5, 10$ GeV respectively.

(b) The relative contribution of the LPM effect in the spectral distribution of emitted photons (see Eq.(41)) Δ_r (per cent). The curves 1, 2, 3, 4 are correspondingly for the electron energies $\varepsilon = 1, 3, 5, 10$ GeV.

We define the contribution of the LPM effect into the radiation spectrum by analogy with [5], as

$$\Delta_r(\varepsilon, y_r) = -\frac{dI(\varepsilon, y_r) - dI^{coh}(\varepsilon, y_r) - dI^{inc}(\varepsilon, y_r)}{dI(\varepsilon, y_r)}. \quad (41)$$

The function $\Delta_r(\varepsilon, y_r)$ is shown in Fig.3(b). It reaches the highest value $\Delta_r = 6.03\%$ at $\varepsilon = 10$ GeV and $y_r = 0.82$. At $\varepsilon = 5$ GeV the maximal value $\Delta_r = 5.84\%$ is attained at $y_r = 0.68$, at $\varepsilon = 3$ GeV the maximal value $\Delta_r = 5.67\%$ is attained at $y_r = 0.56$, and at $\varepsilon = 1$ GeV the maximal value $\Delta_r = 5.41\%$ is attained at $y_r = 0.3$.

All the curves in Fig.3(b) have nearly the same height of the maximum and the position of the maximum y_m and its magnitude are defined roughly by the expressions $u_m \simeq 6\varepsilon/\varepsilon_m$ ($y_m = u_m/(1 + u_m)$), $\Delta_r^{max} \simeq \varepsilon_m^2/(48\varepsilon_g^2)$.

4 Conclusion

In this paper the spectral distribution of electron-positron pair created by photon and the spectral distribution of radiation from high-energy electron moving in an oriented crystal is calculated for intermediate energies (a few GeV for heavy elements and a few tens GeV for germanium). The interplay of the coherent and the incoherent parts of corresponding process is essential for the summary spectrum. Just in this situation the effects of multiple scattering of charged particles appear.

In an oriented crystal at motion of created particles (or the initial electron) near a chain of atoms (an axis) the atom density on the trajectory is much higher than in an amorphous medium. Because of this, the parameter, characterizing the influence of multiple scattering on the pair creation process in a medium in absence of an external field ($\nu_0^2 = \omega/\omega_0$), becomes of the order of unity at relatively low energy (values of ω_0 for tungsten and germanium are given in Table 1). For the radiation process the characteristic energy $\varepsilon_0 = \omega_0/4$. From the other side, due to the high density of atoms on the trajectory of created particles near the axis, the strong electric field of the axis acts on the electron (positron). As a result, with energy increase the pair creation formation length diminishes and the characteristic angles of the process expand. Hence the influence of multiple scattering on the process decreases. So, one has to use the general expression for the pair creation probability, which includes both the crystal effective field (the coherent mechanism) and the multiple scattering (the incoherent mechanism) to study the

pair creation process in oriented crystal [4]. The corresponding expression for the radiation process was obtained in [5].

The two first terms of decomposition of the spectral probability of pair creation $dW(\omega, y)$ over the parameter ν_0^2 give the coherent and the incoherent pair creation probabilities. It should be noted that in the incoherent contribution the influence of the axis field is taken into account. The next terms of the decomposition represent the multiple scattering effect (the LPM effect) in the presence of crystalline field.

Since in an amorphous medium even for heavy elements the LPM effect in pair creation process can be observed only in TeV energy range (see e.g. [3]), the possibility to study this effect in GeV energy range is evidently of the great interest. The same is true for the hard part of the radiation spectrum.

In the present paper the detailed analysis of the spectral properties of the pair creation and radiation processes is performed. The influence of different mechanisms on the general picture of event is elucidated. At high energy $\omega \gg \omega_m$ ($\varepsilon \gg \varepsilon_m$) the influence of the multiple scattering on the process under consideration (the LPM effect) manifests itself for relatively low energy of one of the final charged particles ($\varepsilon_f \sim \varepsilon_m \ll \omega$ (ε)). In this region of spectrum $s_3(r_3) \simeq 0$, $s_2(r_2) \simeq 1$ (see Eqs.(4), (23)), so that one can present Eqs.(3) and (22) in the form

$$\begin{aligned} \frac{dW}{dy} &= s_2(y)R_2(\omega y(1-y)) - s_3(y)R_3(\omega y(1-y)) \simeq R_2(\varepsilon) = R_2(\varepsilon_f), \\ \frac{dI}{d\omega} &= r_2(y_r)R_2\left(\frac{\varepsilon}{u}\right) + r_3(y_r)R_3\left(\frac{\varepsilon}{u}\right) \simeq R_2(\varepsilon - \omega) = R_2(\varepsilon_f), \end{aligned} \quad (42)$$

where we neglect the very small difference of the interpolating functions $g_r(x)$ and $g_p(x)$ ($\sim 1\%$). So we have the scaling (dependence on the fixed combination of kinematic variables) not only for different energies of the initial particles in a given process, but also in the both crossing processes under consideration since this is the same combination $\omega y(1-y) = \varepsilon/u = \varepsilon(\varepsilon - \omega)/\omega$. For this reason at high energy of the initial particles the maximum value of the LPM effect for both processes is defined by the maximum of the function $\Delta_{max} = \Delta(z_m)$, where

$$\Delta(z) = \frac{R_2^{coh}(z) + R_2^{inc}(z)}{R_2(z)} - 1, \quad z_m \simeq \frac{\varepsilon_m}{6}. \quad (43)$$

In the low energy region $\omega(\varepsilon) \leq \omega_m = \varepsilon_m$ this scaling remains only approximate one. Nevertheless the value of maximum and its position vary weakly. Just this energy region is suitable for the experimental study because the

rather wide of spectrum $\Delta y \sim 1$ contributes. It should be emphasized that the LPM effect is large enough for heavy elements only (it is around 8 % in the maximum for tungsten at T=100 K, see Fig.1(b)).

Acknowledgments

The authors are indebted to the Russian Foundation for Basic Research supported in part this research by Grant 06-02-16226.

References

- [1] P. L. Anthony, R. Becker-Szendy, P. E. Bosted *et al*, Phys.Rev.**D 56** (1997) 1373.
- [2] H. D. Hansen, U. I. Uggerhoj, C.C.Biino *et al*, Phys.Rev. **D 69** (2004) 032001.
- [3] V. N. Baier and V. M. Katkov, Phys.Rep. **409** (2005) 261.
- [4] V. N. Baier, and V. M. Katkov, Phys.Lett., **A 346** (2005) 359.
- [5] V. N. Baier, and V. M. Katkov, Phys. Lett.,**A 353** (2006) 91.
- [6] J. U. Andersen, K.Kirsebom, S. P. Moller *et al*, *Electromagnetic Processes in Strong Crystalline Fields*, CERN-SPSC-2005-030.
- [7] V. N. Baier, V. M. Katkov and V. M. Strakhovenko, *Electromagnetic Processes at High Energies in Oriented Single Crystals* (World Scientific Publishing Co, Singapore, 1998).

V.N. Baier and V.M. Katkov

**Opportunity to study
the LPM effect in oriented crystal
at GeV energy**

В.Н. Байер, В.М. Катков

**Возможность изучения ЛПМ эффекта
в ориентированных монокристаллах
при энергии порядка ГэВ**

Budker INP 2007-34

Ответственный за выпуск А.М. Кудрявцев
Работа поступила 21.11.2007 г.

Сдано в набор 22.11.2007 г.

Подписано в печать 23.11.2007 г.

Формат бумаги 60×90 1/16 Объем 1.2 печ.л., 1.0 уч.-изд.л.

Тираж 105 экз. Бесплатно. Заказ № 34

Обработано на IBM PC и отпечатано на
ротапринте ИЯФ им. Г.И. Будкера СО РАН

Новосибирск, 630090, пр. академика Лаврентьева, 11.